Cytogenetic and Genome Research

Original Article

Cytogenet Genome Res 2024;164:23–32
DOI: 10.1159/000539294

Received: April 15, 2024
Accepted: May 8, 2024
Published online: May 16, 2024

Loss of One X and the Y Chromosome Changes the Configuration of the X Inactivation Center in the Genus *Tokudaia*

Luisa Matiz-Ceron[a] Miki Okuno[b] Takehiko Itoh[c] Ikuya Yoshida[a, d] Shusei Mizushima[a, d] Atsushi Toyoda[e, f] Takamichi Jogahara[g] Asato Kuroiwa[a, d]

[a]Reproductive and Developmental Science, Biosystems Science Course, Graduate School of Life Science, Hokkaido University, Sapporo, Japan; [b]Division of Microbiology, Department of Infectious Medicine, Kurume University School of Medicine, Kurume, Fukuoka, Japan; [c]School of Life Science and Technology, Tokyo Institute of Technology, Tokyo, Japan; [d]Division of Reproductive and Developmental Biology, Department of Biological Sciences, Faculty of Science, Hokkaido University, Sapporo, Japan; [e]Comparative Genomics Laboratory, National Institute of Genetics, Mishima, Shizuoka, Japan; [f]Advanced Genomics Center, National Institute of Genetics, Mishima, Shizuoka, Japan; [g]Faculty of Law, Economics and Management, Okinawa University, Naha, Okinawa, Japan

Keywords
Dosage compensation · *Xist* · *Tsix* · X chromosome inactivation · Spiny rat

Abstract

Introduction: X chromosome inactivation (XCI) is an essential mechanism for dosage compensation between females and males in mammals. In females, XCI is controlled by a complex, conserved locus termed the X inactivation center (Xic), in which the lncRNA *Xist* is the key regulator. However, little is known about the Xic in species with unusual sex chromosomes. The genus *Tokudaia* includes three rodent species endemic to Japan. *Tokudaia osimensis* and *Tokudaia tokunoshimensis* lost the Y chromosome (XO/XO), while *Tokudaia muenninki* (TMU) acquired a neo-X region by fusion of the X chromosome and an autosome (XX/XY). We compared the gene location and structure in the Xic among *Tokudaia* species. ***Methods:*** Gene structure of nine genes in Xic was predicted, and the gene location and genome sequences of Xic were compared between mouse and *Tokudaia* species. The expression level of the gene was confirmed by transcripts per million calculation using RNA-seq data. ***Results:*** Compared to mouse, the Xic gene order and location were conserved in *Tokudaia* species. However, remarkable structure changes were observed in lncRNA genes, *Xist* and *Tsix*, in the XO/XO species. In *Xist,* important functional repeats, B-, C-, D-, and E-repeats, were partially or completely lost due to deletions in these species. RNA-seq data showed that female-specific expression patterns of *Xist* and *Tsix* were confirmed in TMU, however, not in the XO/XO species. Additionally, three deletions and one inversion were confirmed in the intergenic region between *Jpx* and *Ftx* in the XO/XO species. ***Conclusion:*** Our findings indicate that even if the *Xist* and *Tsix* lncRNAs are expressed, they are incapable of producing a successful and lasting XCI in the XO/XO species. We hypothesized that the significant structure change in the intergenic region of *Jpx-Ftx* resulted in the inability to perform the XCI, and, as a result, a

karger@karger.com
www.karger.com/cgr

Correspondence to:
Asato Kuroiwa, asatok@sci.hokudai.ac.jp

Karger

lack of *Xist* expression. Our results collectively suggest that structural changes in the Xic occurred in the ancestral lineage of XO/XO species, likely due to the loss of one X chromosome and the Y chromosome as a consequence of the degradation of the XCI system.

Introduction

In Eutheria, females possess two X chromosomes, whereas males carry a single X and a Y chromosome. To address the gene dosage imbalance on the X chromosome between females and males, mammalian cells have evolved a mechanism called X chromosome inactivation (XCI), wherein one of the X chromosomes in females is transcriptionally silenced [1–3]. This process ensures equitable X-linked gene expression levels in somatic cells [4]. The XCI mechanism is governed when the X chromosome-to-autosome ratio (X/A) is ≥1, and one of the X chromosomes is inactivated to achieve a balanced ratio [5].

The mechanism underlying XCI, resulting from the XX/XY constitution, is conserved and widespread among Eutheria. Nevertheless, a few exceptional mammalian species possess unique sex chromosomes, and the genus *Tokudaia* (Muridae, Rodentia) stands out as a prime example. The genus includes three species, each endemic to a single island in southernmost Japan, and is faced with significant conservation challenges [6]. The Tokunoshima spiny rat (*Tokudaia tokunoshimensis* (TTO), $2n = 45$, XO/XO) and Amami spiny rat (*Tokudaia osimensis* (TOS), $2n = 25$, XO/XO) lack one X chromosome and the Y chromosome. The *Sry* gene, a sex-determining gene in eutherian and marsupial mammals, was also completely lost [7–9]. Both males and females share a single X chromosome, and their genome sequences are nearly identical with only a male-specific 34 kb duplication upstream of *Sox9* on chromosome 3 in TOS [10], resulting in equal gene dosage of the X chromosome in the XO/XO species. By contrast, the Okinawa spiny rat (*Tokudaia muenninki* (TMU), $2n = 44$) exhibits the typical XX/XY sex chromosome system found in most mammals [11]. However, the sex chromosomes have fused with a pair of autosomes, forming recently acquired regions referred to as the "neo-X" and "neo-Y" on the X and Y chromosomes, respectively. These neo-X and neo-Y regions display partial genetic differentiation, indicating recombination suppression between them [12].

Transcaucasian mole vole, *Ellobius lutescens* ($2n = 17$), also has been known as an XO/XO species. The closely related species, *Ellobius talpinus*, has a 54,XX karyotype in both females and males, and the XCI mechanism is most likely still intact [13, 14]. The previous report showed that the X remained monovalent without chiasma formation in female and male meiosis in *E. lutescens*, XO/XO [13]. The genome sequencing of Xic in *E. lutescens* indicated that all genes known to control XCI are still present, and the whole region showed >90% conservation between *E. lutescens* and *E. talpinus* [15].

To achieve XCI, a complex interplay of multiple long non-coding RNAs (lncRNAs) and proteins occurs at a pivotal locus known as the X inactivation center (Xic). In both mice and humans, the Xic encompasses an approximately 660 kb region [16]. Within the Xic, critical sequences govern the counting, selection, and initiation of silencing of the future inactive X (Xi), while maintaining gene expression from the active X (Xa) [17]. Several genes reside in the Xic, including the lncRNAs *Tsx* (also known as protein-coding gene [18]), *Xist*, *Tsix*, *Jpx*, and *Ftx*, and protein-coding genes *Cdx4, Chic1, Slc16a2,* and *Rlim*. The cornerstone of XCI regulation is the lncRNA *Xist* [1, 19, 20]. Mouse *Xist* has six conserved repeat sequences, A-, B-, C-, D-, E-, and F-repeats, and two promoters, P1 and P2 [21–26]. These repeats are distributed across exon 1 (A–D and F) and exon 7 (E). The pivotal role of *Xist* in XCI is attributed to the presence of these highly conserved repeats, particularly the A-repeat [27]. *Xist* lacking the A-repeat is expressed but unable to form the characteristic Xi-associated structure due to the lack of initial coiling [28]. The A-repeat includes 7–8 copies of a conserved sequence known as the AUCG tetraloop [29]. The other repeats function as binding sites for chromatin regulatory complexes, loop maintenance, localization, and late stages of XCI [22, 30, 31].

We previously sequenced the *Xist* gene and assessed *Xist* RNA expression and localization in two species with distinct sex chromosome systems, TOS (XO/XO) and TMU (XX/XY) [32]. In TOS, we observed loss-of-function mutations in the *Xist* gene. Notably, RT-PCR and Northern blotting analyses confirmed the absence of *Xist* RNA expression in both male and female TOS cells. By contrast, TMU exhibited female-specific *Xist* RNA expression, with localization predominantly to the long arm of the original X chromosome and partial localization to the neo-X region of Xi [33]. Interestingly, although the neo-X region in TMU does not exhibit heterochromatinization and does not contribute to Barr body formation, it forms a slightly condensed structure [33]. Other genes essential for XCI within the genus *Tokudaia* have not been characterized.

In this study, we compared the Xic structure in three *Tokudaia* species and the mouse model. We detected nine

key genes within the Xic, namely, *Cdx4, Chic1, Tsx, Xist, Tsix, Jpx, Ftx, Rlim,* and *Slc16a2*, in all *Tokudaia* species. Through a detailed sequence comparison, we identified remarkable structural changes in lncRNA genes, *Xist* and *Tsix*, and the intergenic region *Jpx-Ftx* that were specific to the two XO/XO species. Furthermore, transcripts per million (TPM) estimated from RNA-seq data showed female-specific expression of *Xist* and *Tsix* in the XX/XY species, but not in the two XO/XO species. Our findings provide evidence that the lack of XCI in the XO/XO species can be explained by major changes in the Xic, shedding new light on the interplay between sex chromosome evolution and XCI functionality.

Methods

Gene Structure Prediction

The high-quality genome assemblies and gene annotations of the genomes of three *Tokudaia* species were previously reported [34]; however, these annotations do not include ncRNA genes. Therefore, we predicted here the exon-intron structure of nine genes in Xic. We first predicted gene structure for TMU using the following methods: (1) an RNA-seq-based method that predicts gene structures on the basis of transcriptome sequencing results and (2) a homology method that predicts gene structures on the basis of gene sequences of related species, mouse. The two prediction methods are described below.

RNA-Seq-Based Method

Gene prediction was performed using both mapping and de novo methods using RNA-seq data (TMU, DRR059296-302; TTO, DRR496898, DRR496899; and TOS, DRR426688, DRR426689) and genome sequence data [34] (TMU, PRJDB16411; TTO, PRJDB16412; and TOS, PRJDB16413). In the mapping method, HISAT2 v2.2.1 [35] was used to map RNA-seq reads to genome sequences. The mapped reads were assembled into gtf files using StringTie v2.2.1 [36]. In de novo method, RNA-seq reads were used to assemble into transcripts by Trinity v2.9.1 [37]. Redundant sequences were removed from the assembled contigs using CD-Hit v4.8.1 [38], and the contigs were aligned to the genome sequence using GMAP v2023.10.10 [39].

Homology-Based Method

The mouse sequence of each gene (*Cdx4, Chic1, Tsx, Tsix, Xist, Jpx, Ftx, Slc16a2,* and *Rlim*) was used as the query of GMAP v2023.10.10 with cross-species parameter to annotate the TMU genome. Accession numbers of mouse genes are shown in online supplementary Table S1 (for all online suppl. material, see https://doi.org/10.1159/000539294). The gene structure results predicted in TMU were used for the prediction of TTO and TOS genes according to the same methodology.

The prediction results of the two methods were manually curated. For the gene predictions of TTO and TOS, the predicted genes of TMU were aligned to the TTO and TOS genomes by GMAP, partially corrected based on the RNA-seq mapping results.

Xist repeats of *Tokudaia* species were predicted by comparing the sequences of all repeats in mouse [25] to the *Xist* sequence of *Tokudaia* species by using BLAT (v.36) [40]. A customized command was used to improve the sensitivity (blat -noHead -minIdentity = 70 -stepSize = 1 -tileSize = 9).

Comparison of Xic between Mouse and Tokudaia *Species*

To generate the synteny plot of Xic loci, the lylaplot (https://github.com/mokuno3430/emu/tree/main/lyla_plot) tool was used. To run this tool, sequence alignment and comparison were performed by BLAST (v2.9.0) [41]. The mouse Xic genome sequence of mm39 X chromosome (from 5 kb upstream *Cdx4* to 5 kb downstream *Rlim*, 102,360,005-103,029,892) was used for comparison with *Tokudaia* Xic.

Dot plot alignment for pairwise comparison of Xic was generated using the nucmer command in MUMmer (V.3.23) [42]. All output files generated were transformed into matching coordinates by using the mummerplot standard command. The matching coordinate files were plotted using gnuplot (V.5.9) [43].

Gene Expression Analysis

The expression level of genes in Xic was confirmed. The RNA-seq reads were mapped to each species' genome using STAR (v.2.7.9) [44]. Whole genome annotation results were used in which the Xic region was replaced with nine curated transcripts. Then, the TPM was calculated by using RSEM (V.1.3.3) [45] with default parameters for paired-end reads. A bar plot of the TPM per gene was performed using RStudio (V.2012.15.2) [46] and the package ggplot2. TATA box binding protein (*Tbp*) gene was used as an internal control, and its accession number of mouse is shown in online supplementary Table S2.

Results

The Gene Content and Locations in the Xic Are Largely Conserved in Tokudaia *Species*

We compared the gene content and order in the Xic between *Tokudaia* species and mouse. In mouse, *Cdx4, Chic1, Tsx, Tsix, Xist, Jpx, Ftx, Rlim,* and *Slc16a2* were present in the 660 kb Xic (102,365,005–103,024,892 bp from *Cdx4* to *Rlim*) on the X chromosome. All of these genes were annotated to the X chromosome in all *Tokudaia* species and the gene order was conserved (Fig. 1). The estimated lengths of the Xic were 636, 582, and 595 kb in TMU, TTO, and TOS, respectively. Sequence identities between species are shown in Table 1. The sequence identity of *Tokudaia* species and mice was >86%; TTO and TOS showed the highest sequence identity of 99.12%.

Structural Changes in ncRNA Genes

Owing to its importance as the master regulator of XCI, we performed a comparative sequence analysis of *Xist*. We newly determined the *Xist* sequence of TTO and updated the results of a previous study that reported the

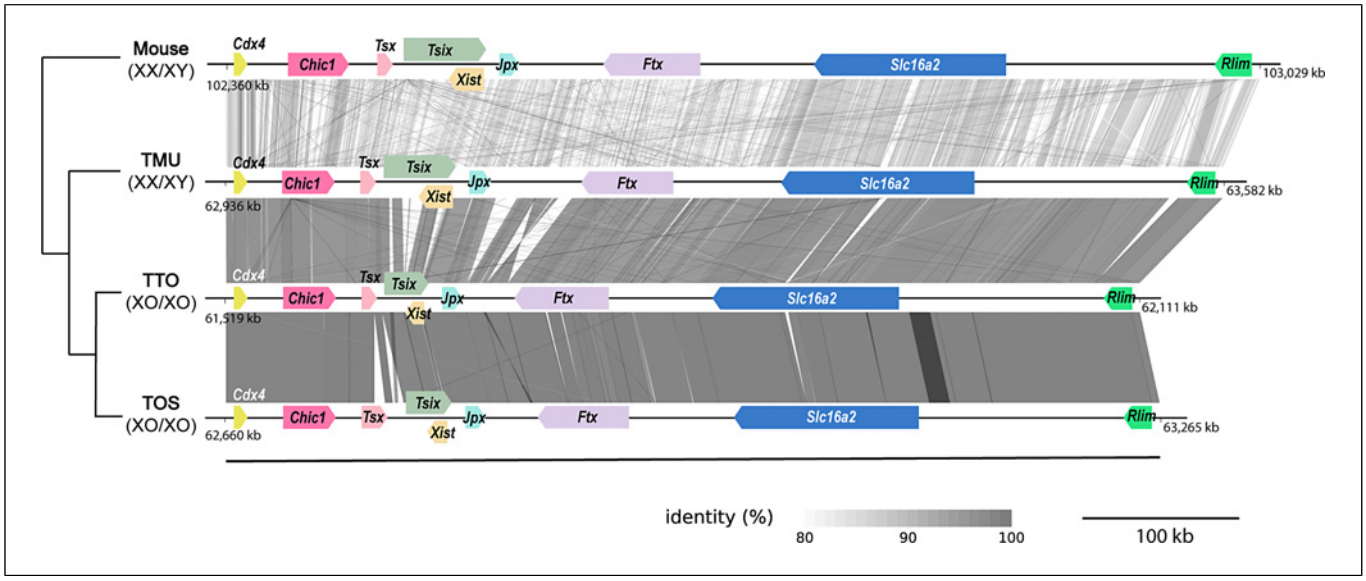

Fig. 1. Xic loci comparison: Gene location and sequence identity in the Xic of mouse, TMU, TOS, and TTO. The lines on the left side mean phylogenetic relationship.

Table 1. Nucleotide sequence identity of the Xic

Species (size of Xic)	Identity, %			
	mouse	TMU	TTO	TOS
Mouse, 660 kb	–	86.62	86.66	86.75
TMU, 636 kb	–	–	96.11	96.01
TTO, 582 kb	–	–	–	99.12
TOS, 595 kb	–	–	–	–

Xist sequences of TMU and TOS [32]. All repeat regions were conserved in TMU, however, with a partial deletion in B- and C-repeat (Fig. 2; Table 2). Although A- and F-repeats were confirmed in TTO and TOS, the D-repeat was completely lost and C- and E-repeats were partially lost as a result of deletions in exons 1 and 7. A partial deletion in B-repeat was confirmed in TOS, but it was completely lost in TTO. *Tsix,* which is the antisense lncRNA to *Xist*, showed significant structural changes in the two XO/XO species (Fig. 3a). The sequence includes mouse exon 3 that was absent in all *Tokudaia* species, and the sequence of exon 2 was additionally lost in the XO/XO species, TTO and TOS.

By comparison of the gene structure between mouse and *Tokudaia* species, *Tokudaia*-specific changes were found in three ncRNA genes, *Tsx*, *Jpx*, and *Ftx* (Fig. 3b–d). Although the sequence of mouse *Tsx* exon 6 was present in all *Tokudaia* genome sequences, it was not transcribed (Fig. 3b). In *Jpx*, the sequence which includes mouse exon 2 was absent in the genome sequence of all *Tokudaia* species (Fig. 3c). The size of exon 3 was longer than that of a mouse; therefore, the total length of exons in *Tokudaia* species is about 800–1,000 bp longer than that of the mouse (online suppl. Table S1). *Ftx* had the same number of exons as a mouse, but with *Tokudaia*-specific features in several exons (Fig. 3d). The sequences of mouse exons 3, 5, and 10 were absent in *Tokudaia* species genomes. The sequences of *Tokudaia* exons 3, 4, and 5 showed the homologies with the mouse exons 4, 6, and 7, respectively. *Tokudaia* exons 6, 7, and 10 were the genus specific sequence. The exon 11 was longer than that of a mouse; therefore, the total length of exons in *Tokudaia* species was about 1,300 bp longer than that of the mouse (online suppl. Table S1). While these changes were observed in ncRNA genes, we confirmed well conservation in protein-coding genes, *Cdx4*, *Chic1*, *Slc16a2*, and *Rlim* (online suppl. Fig. S1; Table S1).

Structural Changes in Xist *and Intergenic Sequence* Jpx-Ftx *in the XO/XO Species*

To visualize detailed Xic structure differences between species, dot plot alignment of all loci in mouse and each *Tokudaia* species was generated (Fig. 4). The dot plot illustrates the high conservation of genomic structure between mouse and TMU in the Xic (Fig. 4a). By contrast, deletions and inversions were identified in TTO and TOS (Fig. 4b, c). We focused on the two regions indicated by gray color in Figures 4b and c, and the enlarged images are shown in Fig. 4d–g. An insertion (6.9 kb) was observed

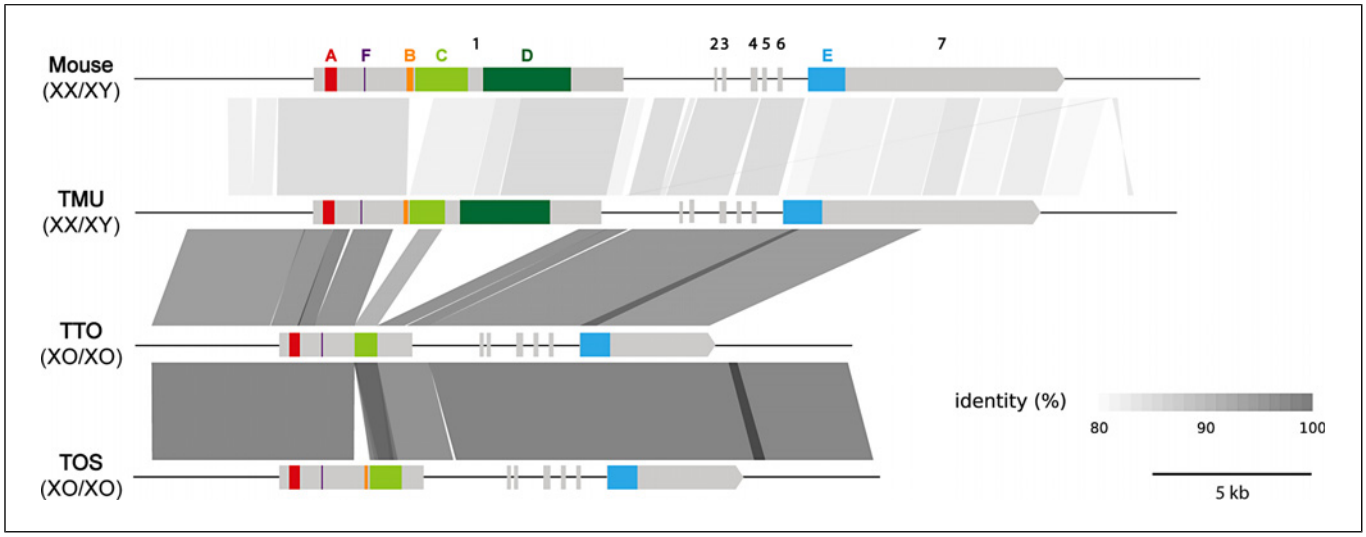

Fig. 2. Gene structure comparison of *Xist*: Comparison of the gene structure of *Xist* in mouse, TMU, TTO, and TOS. Functional repeats of *Xist* are highlighted in color, A (red), F (purple), B (orange), C (yellow-green), D (green), and E (light blue). The number indicates the exon number.

Table 2. Size of *Xist* repeats

Species	Repeats, bp					
	A	F	B	C	D	E
Mouse	365	35	200	1,615	2,700	1,125
TMU	352	36	140	1,079	2,764	1,193
TTO	323	36	0	694	0	913
TOS	324	36	100	978	0	913

in TOS *Tsx* (Fig. 4f), supporting the result of gene structure comparison in Figure 3b. Deletions were confirmed in *Xist and Tsix* (Fig. 4d and f), and these results supported the results in Figures 2 and 3a. Additionally, three deletions and one inversion were confirmed in the intergenic region between *Jpx* and *Ftx* (Fig. 4e, g). The size of each deletion was 10.2 kb, 1.8 kb, and 10.9 kb, and the size of inversion was 11.4 kb. The location and size of deletions and inversion were mostly identical in TTO and TOS.

Expression Levels of Xic Genes Were Affected by the Loss of One X and the Y in XO/XO Species

Since we detected notable structural changes in the two genes, *Xist* and *Tsix*, in the XO/XO species, we estimated TPM values using RNA-seq data to evaluate expression patterns (Fig. 5). The expression levels of *Tbp* as an internal control were mostly the same between sexes in all species (Fig. 5a), supporting the validity of this TPM calculation. TMU *Xist* showed a high female-specific expression, while TTO and TOS showed no expression in either sex (Fig. 5b). We previously reported that the *Xist* lncRNA was not expressed in TOS [32]; therefore, our result supported the previous data. We here newly confirmed that the *Xist* lncRNA was not expressed even in TTO.

Tsix expression was quite low level in TMU (Fig. 5c). The reason for the extremely low expression level of *Tsix* was thought to be that this lncRNA is mainly transcribed in undifferentiated cells such as ES cells [47], and we used differentiated somatic cells (fibroblasts) from each *Tokudaia* species for RNA-seq analysis. Although the expression level was quite low, TMU showed female-specific expression. By contrast, different expression patterns were confirmed in the XO/XO species (Fig. 4c). Neither XO/XO species showed a female-specific expression pattern, suggesting that *Tsix* expression is not regulated in a sex-dependent manner observed in general XX/XY species.

Discussion

We observed that the gene content and order in the Xic are largely conserved between the genus *Tokudaia* and mice, however, with partial structural variation in TTO and TOS. Within *Tokudaia* species, TTO and TOS showed the highest sequence identity. A previous molecular phylogenetic analysis revealed that TMU (XX/XY) diverged first among the three species, and TOS and TTO

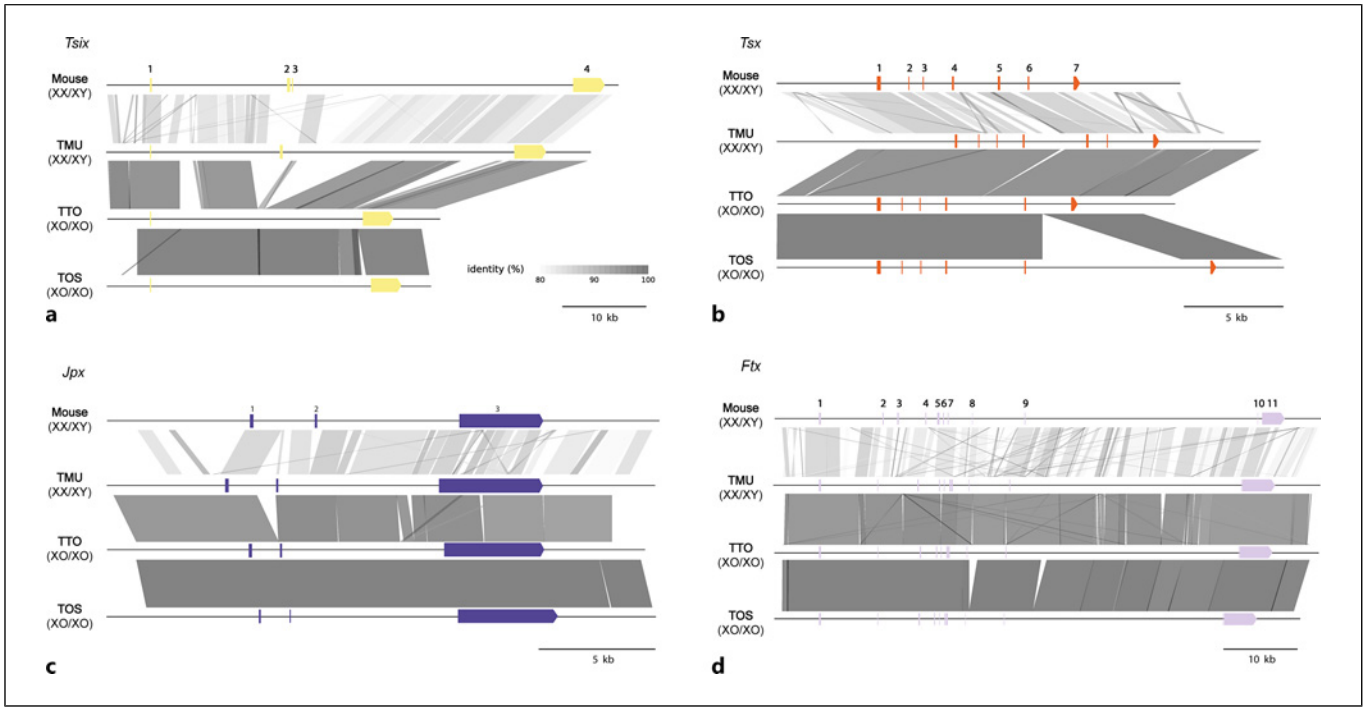

Fig. 3. Gene structure comparison of four ncRNA genes: Comparison of the gene structure of *Tsix* (**a**), *Tsx* (**b**), *Jpx* (**c**), and *Ftx* (**d**) in mouse, TMU, TTO, and TOS. The number indicates the exon number.

(XO/XO) are phylogenetically closely related [9]. Therefore, the patterns of sequence identity likely reflect the phylogenetic relationships within the genus.

Protein-coding genes showed a consistent size and high identity between *Tokudaia* species and mouse, whereas partial variation was discovered in the regions within ncRNA genes. The variation in the three ncRNA genes, *Tsx, Ftx*, and *Jpx*, represent a distinct mark of the *Tokudaia* species, and these variations are not related to sex chromosome constitution.

Only in the XO/XO species, remarkable structure changes were observed in *Xist* and *Tsix* that are a key regulator of XIC and an integral part of its downregulation, respectively. All functional repeats were completely conserved in TMU, suggesting that the *Xist* RNAs of TMU are functionally conserved. This finding supports the results of our previous study of XCI in TMU [32, 33]. By contrast, TTO and TOS exhibited a partial loss of exons 1 and 7, including C-, D-, and E-repeats, and B-repeat is lost in TTO. Notably, the C-repeat recruits the polycomb group complex. Polycomb group works by maintaining the silent state of the Xi through the action of B- and C-repeats [48]. In the same way, the E-repeat is essential for anchoring *Xist* RNA molecules to the Xi territory by facilitating *cis*-localization [49]. The function of the D-repeat is not well-characterized; the region is more heavily degenerated in rodents than in other mammals, suggesting that the mouse D-repeat is not functionally relevant [22, 25]. Based on these previous findings, the deletions in *Xist* in TTO and TOS could affect the recognition and maintenance of the future Xi. The *Xist* lncRNAs are not expressed in the XO/XO species; however, our findings indicate that even if they are expressed, they are incapable of producing a successful and lasting XCI in the XO/XO species. The deletions of *Tsix* in TOS and TTO could also cause XCI regulation failure.

XCI regulatory network is orchestrated by two topologically associating domains (TADs) on the X chromosome, TAD-E and TAD-D, each playing a vital role in governing the XCI process. TAD-E is positioned at the chromosome end, while TAD-D is located closer to the centromere [50]. TAD-E exerts a positive effect, along with *Ftx, Jpx, Rlim*, and *Slc16a2*, on *Xist* production during early development [51, 52]. Conversely, *Rlim* ensures the rapid and stringent inhibition of gene expression in the future Xi [53]. By contrast, TAD-D, which includes *Chic1, Cdx4,* and *Tsx*, participates in negative regulation. *Tsx* and *Tsix,* the latter being the antisense lncRNA to *Xist*, safeguard the future Xa from inactivation by blocking *Xist* coiling on the Xa [18, 54]. Finally, *Chic1* and *Cdx4* contribute to the stabilization of the chromatin

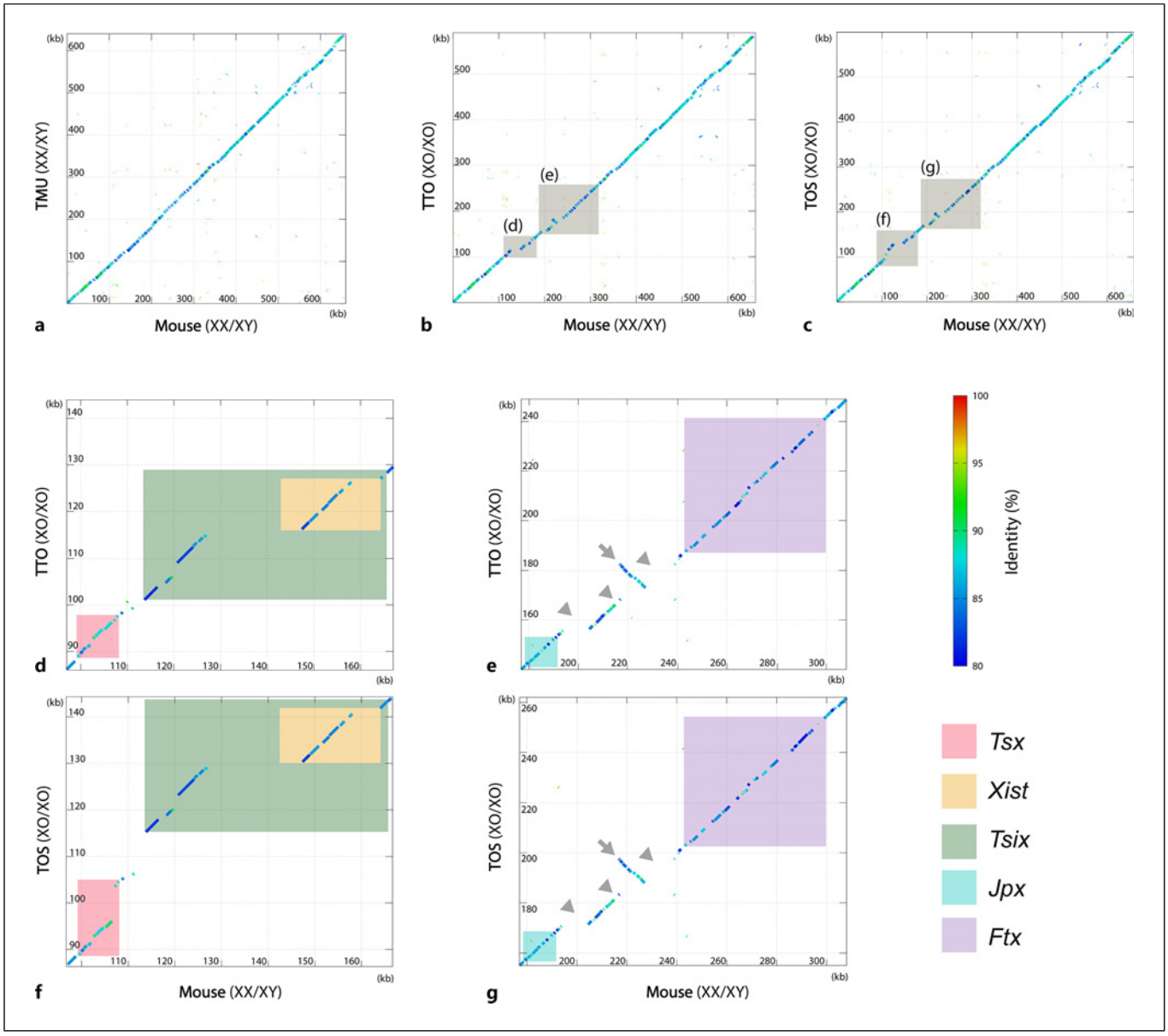

Fig. 4. Dot plot alignment of the Xic: Dot plot alignment between mouse and TMU (**a**), TTO (**b**), and TOS (**c**). Gray squares indicate the misaligned regions. **d**, **f** *Tsx-Xist/Tsix* (**d**, **f**) *Jpx-Ftx* (**e**, **g**) are enlarged views of the regions indicated by gray squares in (**b**) and (**c**), respectively. Arrowheads and an arrow indicate deletions and an inversion in (**e**) and (**g**).

landscape, which is essential for the accurate silencing of the X chromosome [55].

We confirmed large deletions and inversion in the intergenic region of *Jpx-Ftx* in the XO/XO species. The intergenic region of *Jpx–Ftx*, that within TAD-E, upregulates *Xist*. Notably, the loss of the broader *Jpx–Rlim* region reduces XCI [53], emphasizing the significance of this region in mediating chromatin interactions in the Xic. The presence of TADs, including TAD-D and TAD-E, makes essential the interactions between genes and intergenic regions for initiating and maintaining XCI [50]. Successful XCI will create regions of heterochromatin and euchromatin, the latter harboring genes that escape XCI in the Xi [1, 56]. There is evidence that *Ftx* serves as an intermediate in the cascade of events leading from *Rlim* to *Xist* activation [51]. We observed three

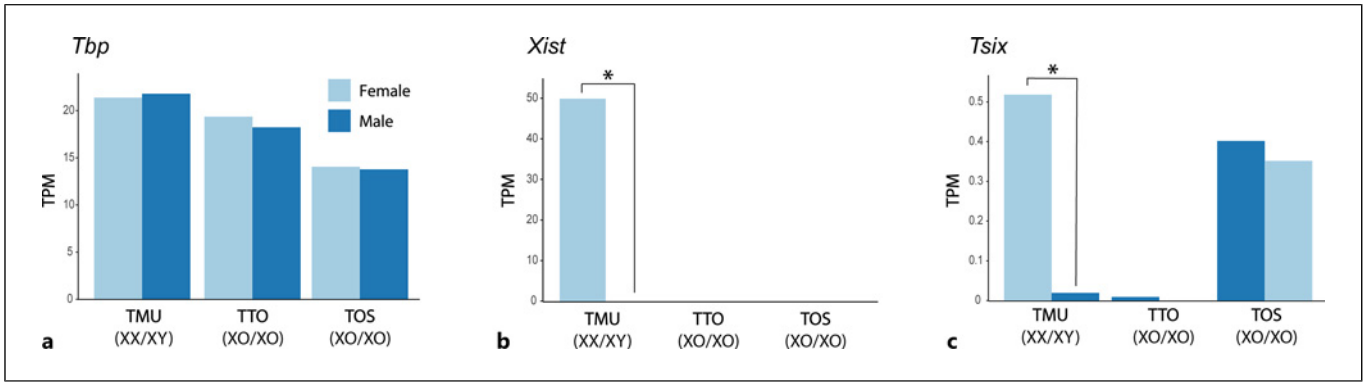

Fig. 5. Expression level of lncRNAs: *Xist* and *Tsix* TPM value of *Tbp* (**a**) as internal control, *Xist* (**b**), and *Tsix* (**c**) in TMU, TTO, and TOS. *$p < 0.05$.

deletions and one inversion in *Jpx-Ftx* in the XO/XO species, both in terms of size and sequence. Mutations in this region likely originated in a common ancestor, raising the possibility that the loss of functional XCI occurred in the ancestral lineage of XO/XO species, likely due to the loss of one X and the Y. We hypothesized that such structural changes would be more likely to occur as a result of having a single X chromosome and self-synapsis. In XO mice, an XO pachytene oocyte in which an unsynapsed univalent X is silenced shows pachytene arrest. By contrast, an XO pachytene oocyte with a self-synapsed X chromosome remains active [57]. Self-synapsis potentially facilitates chromosomal rearrangements. Since it is not possible to obtain tissues from the endangered spiny rat for observations of synapsis, sequence analyses of whole X chromosomes are an important approach to confirm our hypothesis.

The *Xist* lncRNA was not expressed in the XO/XO species, and similarly, female-specific expression of *Tsix* was not observed in them. Since individuals with XX chromosomes have not been confirmed in TOS and TTO, XX is thought to be lethal in the early stages of development due to failure of XCI. We therefore hypothesized that the significant structure changes in the intergenic region of *Jpx-Ftx* resulted in the inability to perform the XCI, and, as a result, a lack of *Xist* expression. To examine whether the deletions and inversion identified here affect TAD formation, we would like to confirm chromatin accessibility using the Hi-C method. Our study marks the first documentation of the Xic structure in XO/XO species. Our findings provide a basis for investigating XCI evolution along with sex chromosome evolution and contribute to a better understanding of the mechanism underlying XCI.

Acknowledgments

The authors would like to thank Yuta Mochimaru and Kentaro Matsuoka (School of Life Science and Technology, Tokyo Institute of Technology) for their valuable work and suggestions to generate the data for this study.

Statement of Ethics

This study did not involve any human participants or specimens. An ethics statement was not required for this study type, and no human or animal subjects were used.

Conflict of Interest Statement

The authors have no conflicts of interest to declare.

Funding Sources

This work was supported by JSPS KAKENHI Grant No. 16H06279 (PAGS), 22H02667, and 23K23930.

Author Contributions

Conceptualization and project administration: A.K. Data curation: L.M.-C. and M.O. Investigation: L.M.-C. Resources: T.-J. Supervision: I.Y., S.M., M.O., T.I., and A.K. Writing and original draft preparation: L.M.-C. and A.K. Writing, review, and editing: L.M.-C., I.Y., S.M., M.O., T.I., and A.K.

Data Availability Statement

The accession numbers of nine genes in Xic of *Tokudaia* species are LC788376-84 (TMU), LC788394-402 (TTO), and LC788385-93 (TOS).

References

1 Loda A, Collombet S, Heard E. Gene regulation in time and space during X-chromosome inactivation. Nat Rev Mol Cell Biol. 2022;23(4):231–49. https://doi.org/10.1038/s41580-021-00438-7
2 Payer B, Lee JT. X chromosome dosage compensation: how mammals keep the balance. Annu Rev Genet. 2008;42(42):733–72. https://doi.org/10.1146/annurev.genet.42.110807.091711
3 Wutz A, Gribnau J. X inactivation Xplained. Curr Opin Genet Dev. 2007;17(5):387–93. https://doi.org/10.1016/j.gde.2007.08.001
4 Lyon MF. Possible mechanisms of X chromosome inactivation. Nat New Biol. 1971;232(34):229–32. https://doi.org/10.1038/newbio232229a0
5 Monkhorst K, de Hoon B, Jonkers I, Mulugeta Achame E, Monkhorst W, Hoogerbrugge J, et al. The probability to initiate X chromosome inactivation is determined by the X to autosomal ratio and X chromosome specific allelic properties. PLoS One. 2009;4(5):e5616. https://doi.org/10.1371/journal.pone.0005616
6 Yamada F, Kawauchi N, Nakata K, Abe S, Kotaka N, Takashima A, et al. Rediscovery after thirty years since the last capture of the critically endangered Okinawa spiny rat Tokudaia muenninki in the northern part of Okinawa island. Mammal Study. 2010;35(4):243–55. https://doi.org/10.3106/041.035.0404
7 Honda T, Suzuki H, Itoh M. An unusual sex chromosome constitution found in the amami spinous country-rat, *tokudaia osimensis osimensis*. Jpn J Genet. 1977;52(3):247–9. https://doi.org/10.1266/jjg.52.247
8 Honda T, Suzuki H, Itoh M, Hayashi K. Karyotypical differences of the amami spinous country-rats, Tokudaia osimensis osimensis obtained from two neighbouring islands. Jpn J Genet. 1978;53(4):297–9. https://doi.org/10.1266/jjg.53.297
9 Murata C, Yamada F, Kawauchi N, Matsuda Y, Kuroiwa A. Multiple copies of SRY on the large Y chromosome of the Okinawa spiny rat, Tokudaia muenninki. Chromosome Res. 2010;18(6):623–34. https://doi.org/10.1007/s10577-010-9142-y
10 Terao M, Ogawa Y, Takada S, Kajitani R, Okuno M, Mochimaru Y, et al. Turnover of mammal sex chromosomes in the Sry-deficient Amami spiny rat is due to male-specific upregulation of Sox9. Proc Natl Acad Sci USA. 2022;119(49):e2211574119. https://doi.org/10.1073/pnas.2211574119
11 Tsuchiya K, Wakana S, Suzuki H, Hattori S, Hayashi Y. Taxonomic study of Tokudaia (Rodentia: muridae): I.genetic differentiation. Mem Natl Sci Mus. 1989;22:227–34.
12 Murata C, Yamada F, Kawauchi N, Matsuda Y, Kuroiwa A. The Y chromosome of the Okinawa spiny rat, Tokudaia muenninki, was rescued through fusion with an autosome. Chromosome Res. 2012;20(1):111–25. https://doi.org/10.1007/s10577-011-9268-6
13 Matveevsky S, Kolomiets O, Bogdanov A, Hakhverdyan M, Bakloushinskaya I. Chromosomal evolution in mole voles Ellobius (cricetidae, Rodentia): bizarre sex chromosomes, variable autosomes and meiosis. Genes. 2017;8(11):306. https://doi.org/10.3390/genes8110306
14 Just W, Baumstark A, Süss A, Graphodatsky A, Rens W, Schäfer N, et al. Ellobius lutescens: sex determination and sex chromosome. Sex Dev. 2007;1(4):211–21. https://doi.org/10.1159/000104771
15 Mulugeta E, Wassenaar E, Sleddens-Linkels E, van IJcken W, Heard E, Grootegoed JA, et al. Genomes of Ellobius species provide insight into the evolutionary dynamics of mammalian sex chromosomes. Genome Res. 2016;26(9):1202–10. https://doi.org/10.1101/gr.201665.115
16 Chureau C, Prissette M, Bourdet A, Barbe V, Cattolico L, Jones L, et al. Comparative sequence analysis of the X-inactivation center region in mouse, human, and bovine. Genome Res. 2002;12(6):894–908. https://doi.org/10.1101/gr.152902
17 Augui S, Nora EP, Heard E. Regulation of X-chromosome inactivation by the X-inactivation centre. Nat Rev Genet. 2011;12(6):429–42. https://doi.org/10.1038/nrg2987
18 Anguera MC, Ma W, Clift D, Namekawa S, Kelleher RJ 3rd, Lee JT. Tsx produces a long noncoding RNA and has general functions in the germline, stem cells, and brain. PLoS Genet. 2011;7(9):e1002248. https://doi.org/10.1371/journal.pgen.1002248
19 Hierholzer A, Chureau C, Liverziani A, Ruiz NB, Cattanach BM, Young AN, et al. A long noncoding RNA influences the choice of the X chromosome to be inactivated. Proc Natl Acad Sci U S A. 2022;119(28):e2118182119. https://doi.org/10.1073/pnas.2118182119
20 Lee J, Davidow LS, Warshawsky D. Tsix, a gene antisense to Xist at the X-inactivation centre. Nat Genet. 1999;21(4):400–4. https://doi.org/10.1038/7734
21 Brown CJ, Hendrich BD, Rupert JL, Lafrenière RG, Xing Y, Lawrence J, et al. The human XIST gene: analysis of a 17 kb inactive X-specific RNA that contains conserved repeats and is highly localized within the nucleus. Cell. 1992;71(3):527–42. https://doi.org/10.1016/0092-8674(92)90520-m
22 Nesterova TB, Slobodyanyuk SY, Elisaphenko EA, Shevchenko AI, Johnston C, Pavlova M, et al. Characterization of the genomic Xist locus in rodents reveals conservation of overall gene structure and tandem repeats but rapid evolution of unique sequence. Genome Res. 2001;11(5):833–49. https://doi.org/10.1101/gr.174901
23 Navarro P, Page DR, Avner P, Rougeulle C. Tsix-mediated epigenetic switch of a CTCF-flanked region of the Xist promoter determines the Xist transcription program. Genes Dev. 2006;20(20):2787–92. https://doi.org/10.1101/gad.389006
24 Pugacheva EM, Tiwari VK, Abdullaev Z, Vostrov AA, Flanagan PT, Quitschke WW, et al. Familial cases of point mutations in the XIST promoter reveal a correlation between CTCF binding and pre-emptive choices of X chromosome inactivation. Hum Mol Genet. 2005;14(7):953–65. https://doi.org/10.1093/hmg/ddi089
25 Raposo AC, Casanova M, Gendrel AV, da Rocha ST. The tandem repeat modules of Xist lncRNA: a swiss army knife for the control of X-chromosome inactivation. Biochem Soc Trans. 2021;49(6):2549–60. https://doi.org/10.1042/BST20210253
26 Sheardown SA, Duthie SM, Johnston M, Newall AET, Formstone EJ, Arkell RM, et al. Stabilization of Xist RNA mediates initiation of X chromosome inactivation. Cell. 1997;91(1):99–107. https://doi.org/10.1016/s0092-8674(01)80012-x
27 Maenner S, Blaud M, Fouillen L, Savoye A, Marchand V, Dubois A, et al. 2-D Structure of the A region of Xist RNA and its implication for PRC2 association. PLoS Biol. 2010;8(1):e1000276. https://doi.org/10.1371/journal.pbio.1000276
28 Schoeftner S, Sengupta AK, Kubicek S, Mechtler K, Spahn L, Koseki H, et al. Recruitment of PRC1 function at the initiation of X inactivation independent of PRC2 and silencing. EMBO J. 2006;25(13):3110–22. https://doi.org/10.1038/sj.emboj.7601187
29 Duszczyk MM, Wutz A, Rybin V, Sattler M. The Xist RNA A-repeat comprises a novel AUCG tetraloop fold and a platform for multimerization. RNA. 2011;17(11):1973–82. https://doi.org/10.1261/rna.2747411
30 Jeon Y, Lee JT. YY1 tethers Xist RNA to the inactive X nucleation center. Cell. 2011;146(1):119–33. https://doi.org/10.1016/j.cell.2011.06.026
31 Sarma K, Levasseur P, Aristarkhov A, Lee JT. Locked nucleic acids (LNAs) reveal sequence requirements and kinetics of Xist RNA localization to the X chromosome. Proc Natl Acad Sci U S A. 2010;107(51):22196–201. https://doi.org/10.1073/pnas.1009785107
32 Zushi H, Murata C, Mizushima S, Nishida C, Kuroiwa A. Unique XCI evolution in Tokudaia: initial XCI of the neo-X chromosome in Tokudaia muenninki and function loss of XIST in Tokudaia osimensis. Chromosoma. 2017;126(6):741–51. https://doi.org/10.1007/s00412-017-0639-4
33 Kudo R, Yoshida I, Matiz Ceron L, Mizushima S, Kuroki Y, Jogahara T, et al. The neo-X does not form a Barr body but shows a slightly condensed structure in the Okinawa spiny rat (Tokudaia muenninki). Cytogenet Genome Res. 2023;162(11–12):632–43. https://doi.org/10.1159/000531275

34 Okuno M, Mochimaru Y, Matsuoka K, Yamabe T, Matiz-Ceron L, Jogahara T, et al. Chromosomal-level assembly of Tokudaia osimensis, Tokudaia tokunoshimensis, and Tokudaia muenninki genomes. Sci Data. 2023;10(1):927. https://doi.org/10.1038/s41597-023-02845-1
35 Kim D, Langmead B, Salzberg SL. HISAT: a fast spliced aligner with low memory requirements. Nat Methods. 2015;12(4):357–60. https://doi.org/10.1038/nmeth.3317.
36 Shumate A, Wong B, Pertea G, Pertea M. Improved transcriptome assembly using a hybrid of long and short reads with StringTie. PLoS Comput Biol. 2022;18(6):e1009730. https://doi.org/10.1371/journal.pcbi.1009730
37 Grabherr MG, Haas BJ, Yassour M, Levin JZ, Thompson DA, Amit I, et al. Full-length transcriptome assembly from RNA-Seq data without a reference genome. Nat Biotechnol. 2011;29(7):644–52. https://doi.org/10.1038/nbt.1883
38 Li W, Godzik A. Cd-hit: a fast program for clustering and comparing large sets of protein or nucleotide sequences. Bioinformatics. 2006;22(13):1658–9. https://doi.org/10.1093/bioinformatics/btl158
39 Wu TD, Watanabe CK. GMAP: a genomic mapping and alignment program for mRNA and EST sequences. Bioinformatics. 2005;21(9):1859–75. https://doi.org/10.1093/bioinformatics/bti310
40 Kent WJ. BLAT: the BLAST-like alignment tool. Genome Res. 2002;12(4):656–64. https://doi.org/10.1101/gr.229202
41 Altschul SF, Gish W, Miller W, Myers EW, Lipman DJ. Basic local alignment search tool. J Mol Biol. 1990;215(3):403–10. https://doi.org/10.1016/S0022-2836(05)80360-2
42 Delcher AL, Phillippy A, Carlton J, Salzberg SL. Fast algorithms for large-scale genome alignment and comparison. Nucleic Acids Res. 2002;30(11):2478–83. https://doi.org/10.1093/nar/30.11.2478
43 Vaught A. Graphing with Gnuplot and Xmgr: two graphing packages available under linux. Linux J; 1996.
44 Dobin A, Davis CA, Schlesinger F, Drenkow J, Zaleski C, Jha S, et al. STAR: ultrafast universal RNA-seq aligner. Bioinformatics. 2013;29(1):15–21. https://doi.org/10.1093/bioinformatics/bts635
45 Li B, Dewey CN. RSEM: accurate transcript quantification from RNA-Seq data with or without a reference genome. BMC Bioinformatics. 2011;12:323. https://doi.org/10.1186/1471-2105-12-323
46 RStudio: Integrated development environment for R. Available from: http://www.posit.co/ (2006). Accessed Nov 10, 2023.
47 Mise N, Goto Y, Nakajima N, Takagi N. Molecular cloning of antisense transcripts of the MouseXistGene. Biochem Biophys Res Commun. 1999;258(3):537–41. https://doi.org/10.1006/bbrc.1999.0681
48 Bousard A, Raposo AC, Żylicz JJ, Picard C, Pires VB, Qi Y, et al. The role of Xist-mediated Polycomb recruitment in the initiation of X-chromosome inactivation. EMBO Rep. 2019;20(10):e48019. https://doi.org/10.15252/embr.201948019
49 Ridings-Figueroa R, Stewart ER, Nesterova TB, Coker H, Pintacuda G, Godwin J, et al. The nuclear matrix protein CIZ1 facilitates localization of Xist RNA to the inactive X-chromosome territory. Genes Dev. 2017;31(9):876–88. https://doi.org/10.1101/gad.295907.117
50 Van Bemmel JG, Galupa R, Gard C, Servant N, Picard C, Davies J, et al. The bipartite TAD organization of the X-inactivation center ensures opposing developmental regulation of Tsix and Xist. Nat Genet. 2019;51(6):1024–34. https://doi.org/10.1038/s41588-019-0412-0
51 Chureau C, Chantalat S, Romito A, Galvani A, Duret L, Avner P, et al. Ftx is a non-coding RNA which affects Xist expression and chromatin structure within the X-inactivation center region. Hum Mol Genet. 2011;20(4):705–18. https://doi.org/10.1093/hmg/ddq516
52 Tian D, Sun S, Lee JT. The long noncoding RNA, Jpx, is a molecular switch for X-chromosome inactivation. Cell. 2010;143(3):390–403. https://doi.org/10.1016/j.cell.2010.09.049
53 Barakat TS, Gunhanlar N, Pardo CG, Achame EM, Ghazvini M, Boers R, et al. RNF12 activates Xist and is essential for X chromosome inactivation. PLOS Genet. 2011;7(1):e1002001. https://doi.org/10.1371/journal.pgen.1002001
54 Lee JT. Disruption of imprinted X inactivation by parent-of-origin effects at Tsix. Cell. 2000;103(1):17–27. https://doi.org/10.1016/s0092-8674(00)00101-x
55 Hwang JY, Choi KH, Lee DK, Kim SH, Kim EB, Hyun SH, et al. Overexpression of OCT4A ortholog elevates endogenous XIST in porcine parthenogenic blastocysts. J Reprod Dev. 2015;61(6):533–40. https://doi.org/10.1262/jrd.2015-017
56 Fang H, Disteche CM, Berletch JB. X inactivation and escape: epigenetic and structural features. Front Cell Dev Biol. 2019;7:219. https://doi.org/10.3389/fcell.2019.00219
57 Burgoyne PS, Mahadevaiah SK, Turner JMA. The consequences of asynapsis for mammalian meiosis. Nat Rev Genet. 2009;10(3):207–16. https://doi.org/10.1038/nrg2505